Modelling climate change responses in tropical forests: similar productivity estimates across five models, but different mechanisms and responses.

Lucy Rowland[1], Anna Harper[2], Bradley O. Christoffersen[1,3], David R. Galbraith[4], Hewlley M. A. Imbuzeiro[5], Thomas L. Powell[6], Chris Doughty[7], Naomi M. Levine[8], Yadvinder Malhi[7], Scott R. Saleska[3], Paul R. Moorcroft[6] , Patrick Meir[1,9], and Mathew Williams[1].

[1] {School of GeoSciences, University of Edinburgh, Edinburgh, United Kingdom}

[2]{College of Engineering, Mathematics, and Physical Science, University of Exeter, Exeter, United Kingdom}

[3]{Department of Ecology and Evolutionary Biology, University of Arizona, Tucson, Arizona, USA}

[4]{School of Geography, University of Leeds, Leeds, United Kingdom}

[5]{Grupo de Pesquisas em Interação Atmosfera-Biosfera, Universidade Federal de Viçosa, Minas Gerias, Brazil}

[6]{Department of Organismic and Evolutionary Biology, Harvard University, Cambridge, Massachusetts, USA}

[7]{Environmental Change Institute, School of Geography and the Environment, University of Oxford, Oxford, United Kingdom}

[8]{Department of Biological Sciences, University of Southern California, Los Angeles, CA, USA}

[9]{Research School of Biology, Australian National University, Canberra, ACT 2601, Australia}

Abstract

Accurately predicting the response of Amazonia to climate change is important for predicting climate change across the globe. Changes in multiple climatic factors simultaneously result in complex non-linear ecosystem responses, which are difficult to predict using vegetation models. Using leaf- and canopy-scale observations, this study evaluated the capability of five vegetation models (CLM3.5, ED2, JULES, SiB3, and SPA) to simulate the responses of leaf- and canopy-scale productivity to changes in temperature and drought in an Amazonian forest.

The models did not agree as to whether gross primary productivity (GPP) was more sensitive to changes in temperature or precipitation, but all the models were consistent with the prediction that GPP would be higher if tropical forests were 5°C cooler than current ambient temperatures. There was greater model-data consistency in the response of net ecosystem exchange (NEE) to changes in temperature than in the response to temperature by net photosynthesis (A_n), stomatal conductance (g_s) and leaf area index (LAI). Modelled canopy-scale fluxes are calculated by scaling leaf-scale fluxes using LAI. At the leaf-scale, the models did not agree on the temperature or magnitude of the optimum points of A_n, V_{cmax} or g_s, and model variation in these parameters was compensated for by variations in the absolute magnitude of simulated LAI, and how it altered with temperature.

Across the models, there was, however, consistency in two leaf-scale responses: 1) change in A_n with temperature were more closely linked to stomatal behaviour than biochemical processes; and 2) intrinsic water use efficiency increased with temperature, especially when combined with drought. These results suggest that even up to fairly extreme temperature increases from ambient levels (+6˚C), simulated photosynthesis becomes increasingly sensitive to g_s and remains less sensitive to biochemical changes. To improve the reliability of simulations of the response of Amazonian rainforest to climate change, the mechanistic

underpinnings of vegetation models need to be validated at both leaf- and canopy-scales to improve accuracy and consistency in the quantification of processes within and across an ecosystem.

1 Introduction

Continuing increases in atmospheric CO_2 are likely to cause increases in temperature and changes in precipitation across Amazonia (Good et al., 2013; Jupp et al., 2010; Malhi et al., 2009; Marengo et al., 2012). However, significant uncertainty remains regarding the response of tropical forests to warming (Corlett, 2011; Reed et al., 2012; Wood et al., 2012), altered precipitation (Meir et al., 2008; Meir and Woodward, 2010) and short-term abrupt changes in both precipitation and temperature (Cox et al., 2008; Marengo et al., 2011; Reichstein et al., 2013). Such uncertainties are propagated into models, resulting in substantial variability in modelled responses to changes in temperature and drought (Friedlingstein et al., 2006; Galbraith et al., 2010; Powell et al., 2013; Sitch et al., 2008). These responses need to be rigorously assessed to enable further improvement in our ability to predict the impacts of climate change on rain forest functioning.

The ecosystem responses of models to multi-factor changes in climate can be difficult to interpret because of complex nonlinear responses (Zhou et al., 2008), which can vary substantially between vegetation models with different model structures. Previous modelling analyses have shown a greater sensitivity of carbon storage in Amazonian forests to increased temperature than reduced precipitation (Galbraith et al., 2010). However model responses to simultaneous changes in precipitation and temperature complex are difficult to evaluate due to the compound effect of drought and temperature responses (Luo et al., 2008). There are particular challenges when considering short-to-medium term responses (Luo et al., 2008) linked to climatic extremes, such as severe drought (Cox et al., 2008; Marengo et al., 2011).

Concurrent changes in temperature and precipitation can cause a complex chain of positive

and negative feedbacks on different timescales (Figure 1). Increased temperature and reduced precipitation can directly affect stomatal conductance (g_s) through increasing vapour pressure deficit (VPD), or indirectly affect g_s on longer time-scales through reducing soil water content (SWC; Figure 1). Stomatal conductance, g_s, limits photosynthesis (A_n), and therefore gross primary productivity (GPP). However A_n can also be limited by changes in leaf biochemistry (V_{cmax} and J_{max}, Figure 1). How A_n is limited by temperature increase is important as changes in leaf biochemistry at very high temperatures can result from permanent alteration and possible damage to proteins, whereas changes in g_s are less permanent, but alter water use, and potentially water use efficiency. Currently there is no consensus on how A_n will respond to temperature: some studies find a direct impact through leaf biochemistry (Doughty, 2011; Doughty and Goulden, 2008), and others an indirect effect initiated by changes in g_s, because the limitation of increasing VPD on g_s occurs at lower temperatures than those that cause protein damage (Lloyd and Farquhar, 2008). The lack of data for tropical trees means these responses remain poorly constrained, though drought and warming can be examined using limited field data from drought and warming experiments (da Costa et al., 2014; da Costa et al. 2010; Nepstad et al., 2002) and from extreme events within the natural range of the climate (Marengo et al., 2011).

The response of vegetation models to temperature change or drought occurs through the aggregated changes in finer scale processes, for example at the leaf level. Correctly simulating the mechanisms at the leaf scale is therefore important to maintain confidence in canopy-scale predictions. Leaf-scale responses in models are scaled using LAI to simulate the processes at the canopy-scale; therefore inaccuracies in both leaf-scale fluxes and how they are scaled can produce substantial errors in ecosystem scale fluxes (Bonan et al., 2012).

73 Currently no model-data comparisons exist that allow for the evaluation of combined
74 temperature and precipitation/drought sensitivity of ecosystem fluxes in relation to LAI and
75 leaf-scale processes in tropical forests. However if we are to identify accurately how to
76 improve simulated responses of Amazonian forests to future climate change it is vital that
77 model output is evaluated against data from the leaf to the canopy-scale .

78 At the Tapajós national forest in north east Brazil, Doughty and Goulden (2008) collected
79 data on the response of net ecosystem exchange (NEE) to change in atmospheric temperature
80 and the response of A_n and g_s to short-term artificial leaf warming. Doughty and Goulden
81 (2008) found reductions in forest productivity at air temperatures above 28˚C, which
82 corresponds to significant reductions in A_n and g_s at leaf temperatures above 30-33˚C. They
83 suggested that tropical forests may therefore already be close to a temperature threshold,
84 beyond which productivity will decline.

85 Here we use the data published by Doughty and Goulden (2008) to evaluate the short-term
86 temperature responses within models at both the leaf and canopy-scale and investigate how
87 the model formulations might impact predicted responses to multiple climatic factors. Our
88 model simulations represent short-term non-equilibrium responses to changes in temperature
89 to make them comparable to the perturbation data collected by Doughty and Goulden (2008).
90 Evaluation of non-equilibrium changes in models is valuable for assessing how models will
91 perform when simulating responses to extreme shifts in temperature and precipitation which
92 are predicted to increase across Amazonia (Cox et al., 2008; Marengo et al., 2011). If the
93 models were run their equilibrium response to a simulated climate shift, the changes in some
94 of the key variables in the study (A_n, g_s) are more likely to be dominated by the effect of long-

term soil drying rather than direct temperature responses (e.g. the dashed lines in Fig. 1). This study is part of a wider model inter-comparison project which aims to explore how well vegetation models simulate drought in the eastern Amazon (Powell et al., 2013). In this study we evaluate: 1) how the forest productivity of five vegetation models (CLM3.5, ED2, JULES, SiB3, SPA) responds to changes in temperature, 2) what leaf-scale processes drive canopy-scale changes in productivity and 3) how both leaf- and canopy-scale temperature sensitivities are influenced by concurrent changes in precipitation at the Tapajós forest site in eastern Brazil. In all models we simulate first an ambient and then a 50 % reduction in the incoming precipitation during the wet season from 2000-2006 analogous to the drought treatment imposed at the Tapajós forest site, linked to a -5˚C, 0˚C, +2˚C, +4˚C, and +6˚C change to the ambient air temperature (T_{air}). These simulations cover a range of likely and possible increases in temperature for the Amazon region in the coming century (Christensen et al, 2007; Collins et al., 2013; Malhi et al., 2009) and can be evaluated against existing data from Doughty and Goulden (2008). This study is the first to evaluate, using data, the inter-model variability in the leaf and canopy responses to changes in temperature and precipitation at a tropical forest site.

2 Materials and Methods

2.1 Model description

The five models used in this study were the Community Land Model version 3.5 coupled to the Dynamic Global Vegetation model (CLM3.5-DGVM; hereafter CLM3.5), the Ecosystem

116 Demography model version 2 (ED2) , the Joint UK Land Environment Simulator version 2.1
117 (JULES), the Simple Biosphere model version 3 (SiB3), and the Soil-Plant-Atmosphere
118 model (SPA). A brief description of each of the models is given here and in Table 1 (also see
119 Powell et al., (2013)). The simplest canopy structure is in SiB3. SiB3 has a fixed LAI and
120 uses a big-leaf model which simulates the response of the top canopy and integrates this
121 response throughout the canopy according to a light and leaf nitrogen (N) extinction
122 coefficient (Baker et al., 2008; Sellers et al., 1992; Sellers et al., 1996). CLM3.5 is also a big-
123 leaf model, however it separates the canopy into a sunlit leaf fraction (leaves which receive
124 both direct and diffuse light) and a shaded leaf fraction (leaves which receive only diffuse
125 light), which change dynamically with sun angle and canopy light penetration (Oleson et al.,
126 2004; Oleson et al., 2008). The version of JULES used in this study simulates 10 canopy
127 layers with equal leaf area increments. Leaf nitrogen decays exponentially through the
128 canopy and radiation interception is simulated following the two-stream approximation of
129 Sellers (1985). SPA also has a layered canopy model, and here used three canopy layers, with
130 separate sunlit and shaded fractions (Williams, 1996; Williams et al., 2005). ED2
131 mathematically approximates the properties of an individual-based forest gap model,
132 separately modelling the stems of three successional stages (pioneer, mid-successional and
133 late-successional) of, in this study, tropical trees and grasses on a continuum of leaf light
134 levels from fully shaded to fully sunlit (Kim et al., 2012; Medvigy et al., 2009b; Moorcroft et
135 al., 2001). SiB3 and SPA simulate only 1 plant functional type (PFT), set to tropical
136 evergreen broadleaf; JULES and CLM3.5 simulate 5 PFT's, but this site simulated a
137 fractional cover > 95% evergreen broadleaf trees. As the focus of this study is the responses
138 within tropical forests, results were not considered if a model simulated a shift in the PFT

139 away from the dominance of tropical forest.

140 All of the models use enzyme-kinetic A_n equations, derived from Farquhar et al. (1980),
141 Farquhar and Sharkey (1982), Kirschbaum and Farquhar (1984) and Collatz et al. (1991). In
142 all models temperature can affect A_n directly through temperature response functions on the
143 maximum rate of carboxylation of RuBP (V_{cmax}), the CO_2 compensation point, and the
144 Michaelis-Menten constants (K_c and K_o), and in SPA the maximum rate of electron transport
145 (J_{max}). Temperature can also indirectly change A_n through changing the VPD at the leaf
146 surface, which alters g_s. CLM3.5, ED2 and SiB3 use the Ball-Berry stomatal conductance
147 model (Collatz et al., 1991). JULES calculates g_s by relating the ratio of internal to external
148 CO_2 to the humidity deficit (Cox et al., 1998). SPA is unique in that it models stomatal
149 conductance by simulating an aqueous continuum between the soil and leaf water: g_s and
150 photosynthesis are maximised using an isohydric assumption that at each time-step leaf water
151 potential does not drop below a critical level (-2.5 MPa; see Williams et al., 1996, Fisher et
152 al., 2007). CLM3.5, ED2, SiB3 and JULES alter g_s using a water stress factor (β; a value
153 ranging 0-1 where 1 indicates no soil water stress and 0 indicates complete soil water
154 limitation). A detailed description of the effect of soil water stress on g_s and A_n in these
155 models is given by Powell et al., (2013).

156

157 **2.2 Site**

158 The throughfall exclusion in the Tapajós National Forest (TNF, 2.897 S, 54.952 W) is located
159 on an Oxisol soil, and has a mean annual precipitation of approximately 2 m per year; the site

160 is described in detail by Nepstad et al. (2002). This plot was selected for this experiment
161 because on the temperature response of canopy level net ecosystem exchange (NEE) was
162 collected at a nearby site (km83; Doughty and Goulden, 2008). The canopy NEE
163 measurements were from an eddy covariance tower from July 2000 to July 2001, when light
164 levels were above 1000 μmol m^{-2} s^{-1} (Doughty and Goulden, 2008). Leaf level responses of
165 stomata conductance and photosynthesis to increases in leaf temperature in fully sunlit
166 canopy leaves were from 3 species in 2004 (see Doughty and Goulden, 2008 and Goulden et
167 al., 2004).

168

169 **2.3 Meteorological Data and Soil Properties**

170 The model simulations were driven using hourly meteorological data (precipitation, T_{air},
171 specific humidity, short and long-wave radiation and air pressure) measured above the
172 canopy at the site from 01/01/2002-31/12/2004. The short-wave radiation was split into 68%
173 direct and 32% diffuse, and then this was split into 43% visible and 57% near-infrared for
174 direct, and 52% visible and 48% near-infrared for diffuse (Goudriaan, 1977).

175 The soil properties were standardised across all models to create a similar soil physical
176 environment, thereby testing only for differences in vegetation functioning (see Powell et al.,
177 2013). Only biological properties such as rooting depth, root biomass, as well as the total
178 number of soil layers were left as model specific soil properties.

179

2.4 Experimental design

All of the models went through a standard spin-up procedure prior to simulations (see Powell et al., 2013). Following the spin-up period, a series of five model simulations, with varying T_{air}, were performed for an eight-year period (which was intended to simulate 1999-2006, see Powell et al., 2013) for ambient precipitation (control simulations) and for simulations with a 50 % reduction in wet season rainfall (drought simulations). The 2002-2004 meteorological data were recycled over the eight year simulation period. To explore the effects of changes in T_{air} on the models we performed five model simulations which consisted of simulations with the hourly 2000-2006 ambient T_{air} adjusted by -5˚C, 0 ˚C (ambient T_{air}), +2˚C, +4˚C and +6˚C. 1999 was the baseline year for which no changes from ambient temperature and precipitation were implemented. Our analysis was focused on increases in temperature; however we included a simulation with temperatures 5 ˚C lower than ambient temperatures, on the basis that some models may have processes optimised for temperate regions where average T_{air} is lower. VPD was adjusted according to the changes in air temperature.

2.5 Model output and evaluation

All the data in this study was processed to match the collection methods and processing done by Doughty and Goulden (2008; hereafter referred to as DG), as closely as possible. Therefore, to compare the models' predictions NEE with the flux data, we extract canopy level fluxes when photosynthetic photon flux density (PPFD) was > 1000 μmol m^{-2} s^{-1}, the conditions used by DG. PPFD was not available for the whole period; therefore we use the

measured shortwave radiation to estimate PPFD. A conversion factor of 2 is used to convert from shortwave radiation (W m^{-2}) to PPFD (μmol m^{-2} s^{-1}) based on an empirical relationship calculated from the flux tower at the study site (Doughty, unpublished data). The results on hourly time-steps from each model for the period of (2000-2006) for the five temperature simulations (with offset of -5˚C, +0˚C, +2˚C, +4˚C and +6˚C) were pooled. Model output was then placed into 1 ˚C bins of T_{air} for the canopy-scale analysis (GPP, NEE, ecosystem respiration (R_{eco})) or of leaf temperature (T_{leaf}), for leaf-scale analysis, as done in the DG study. Accounting for non-gaussian distributions in model output the median and the 15.9^{th} and 84.1^{th} quantiles of the binned model output are plotted to represent the mean and 1 standard deviation of the temperature response curve of any model variable. The data from the drought and control simulations are considered separately.

To explore the relative sensitivity of models to changes in temperature and drought a linear relationship between the temperature increase per control simulation (-5 ˚C, 0 ˚C, 2 ˚C, 4 ˚C, 6 ˚C) and final year (2006) GPP was used to calculate the change in GPP per 1˚C increase T_{air} for each model (Table 2). This value was used to calculate the increase in temperature necessary to produce the same loss of GPP as the ambient T_{air} drought simulation, where there is a 50% reduction in wet season rainfall (Table 2).

DG published data for the temperature response of A_n and g_s of sunlit leaves during the dry season when PPFD is >1000 μmol m^{-2} s^{-1}. CLM3.5 and SPA are the only models which have separate output for sunlit and shaded leaves. Consequently data from the sunlit leaves of these models from periods of high PPFD (>1000 μmol m^{-2} s^{-1}) during the dry season (July-December) were used for comparison. The effect of increasing T_{air} reducing modelled soil

223 water content (via increased VPD and consequent leaf transpiration) had to be removed from
224 the model outputs to make it comparable to the DG data, where individual leaves were
225 artificially warmed. Therefore we only selected model outputs from the temperature
226 simulations if the soil water content in the rooting zone was in the top quartile of the values
227 from the ambient control simulation, this corresponded to β values of >0.9 in CLM3.5. For
228 consistency with the sunlit leaf analysis, the analysis of canopy average leaf data from all
229 models was done using dry season data with PPFD >1000 μmol m^{-2} s^{-1}.

230 The relative sensitivity of the five models to changes in temperature and precipitation is
231 assessed by comparing the interactive and non-interactive effects of the 50 % reduction in
232 wet season precipitation (drought simulation) with the -5˚C, 0, and +6˚C change in T_{air} on
233 ecosystem fluxes at the end of the 8 year simulation (2006).

234

235 **3 Results**

236 **3.1 Canopy-scale responses**

237 The models have similar responses of NEE and GPP to increasing T_{air}. DG observed a
238 reduction in carbon uptake as NEE went from -17.4±0.3 to -7.9±1.1 μmol m^{-2} s^{-1},
239 corresponding to an increase in T_{air} from 28˚C - 32˚C (Figure 2a). The modelled NEE begins
240 to increase at a lower T_{air} (22-25˚C) in the models and the 28˚C - 32˚C increase in NEE is
241 generally substantially less than observed by DG (2.5-3.9 μmol m^{-2} s^{-1}), except in SPA which
242 experiences a similar increase in NEE as DG from 28˚C - 32˚C (8.8 μmol m^{-2} s^{-1}), across the
243 same range of values (-15.8 to -7.0 μmol m^{-2} s^{-1}; Figure 2a). The increase in modelled NEE at

244 high temperatures is caused by a decline in GPP across all models (Figure 2b). As T_{air}
245 increases from 16˚C to 38˚C the average decline in GPP from all models is 20.9±3.2 μmol m^{-2}
246 s^{-1}. In contrast the mean model decline in R_{eco} over the same modelled T_{air} range was
247 4.2±1.8 μmol m^{-2} s^{-1} (Figure 2c). The decline in modelled ecosystem respiration is low
248 because in all models a decline in autotrophic respiration with increasing temperature (linked
249 in the models with reduced GPP) is opposed by an increase in heterotrophic respiration (data
250 not shown).

251 Declines in GPP corresponded to declines in LAI. Between 25˚C to 38˚C the decline in GPP
252 in CLM3.5 (89±38 %), and SPA (82±26 %) was greater than in other models (Figure 2b) and
253 matched by greater declines in LAI over the same temperature range (4.2±1.0 m^2 m^{-2},
254 CLM3.5 and 4.4±0.9 m^2 m^{-2} in SPA, relative to only 0.6±0.3 m^2 m^{-2} in ED2 and 0.4±0.1 m^2
255 m^{-2} in JULES; Figure 2d). The inter-model variability in LAI is large; at 25 ˚C the median
256 LAI value in ED2 (3.6±0.3 m^2 m^{-2}) is 3 times smaller than the median values in CLM3.5
257 (10.7±1.0 m^2 m^{-2}). Observed mean LAI at the TNF under non-drought conditions ranged
258 from 5.5-6.3 m^2 m^{-2} from 2000 to 2005 (Brando et al., 2008) and therefore the modelled
259 values span a range ~70% above and below the measured LAI (Figure 2d).

260 Combined drought and warming had compound effects on GPP, R_{eco}, and LAI. In CLM3.5
261 GPP remained the same in the T_{air} -5˚C simulation at the end of the drought and control
262 simulation, however in the T_{air} +6˚C simulation the forest which existed at the end of the
263 control simulation was replaced with grassland in the drought simulation (GPP values for
264 grassland are not shown, Figure 3a). In JULES, SiB3 and SPA the GPP was the same in the
265 control and the drought simulation at T_{air} -5˚C; however GPP is 61%, 58% and 44% lower

266 respectively at the end of the drought relative to the control simulation (Figure 3a). The
267 combined effect of temperature and drought on GPP and R_{eco} is lowest in ED2, because it
268 was the only model to have a strong drought effect on GPP, R_{eco} and LAI in the T_{air} -5˚C
269 simulation (Figure 3). In CLM3.5 and SPA, GPP and LAI have the same fractional
270 reductions with drought, at higher temperatures (Figure 3a and 3c), indicating a tight
271 coupling between the LAI and canopy productivity; this contrasts the lack of, or low GPP-
272 LAI feedback in SiB3 and JULES.

273 Amongst the models there is a continuum of temperature versus drought sensitivity. We
274 express the temperature versus drought sensitivity as the equivalent temperature increase
275 necessary to produce the same GPP reduction as between the last year of the control to the
276 drought simulation at ambient T_{air} (Table 2). A low equivalent temperature would represent a
277 greater GPP sensitivity to temperature increase and/or a lower GPP sensitivity to drought; a
278 higher equivalent temperature represents a lower GPP sensitivity to temperature increase
279 and/or a higher GPP sensitivity to drought. The equivalent temperature increase necessary to
280 reproduce the same GPP reduction as from the last year of control and droughts simulation at
281 ambient temperature was lowest in SPA (4.92˚C), moderate in JULES and CLM3.5 (8.61˚C
282 and 8.83˚C, respectively), and highest in SiB3 and ED2 (15.70˚C and 17.50˚C, respectively;
283 Table 2). However across all the models a 5˚C reduction in ambient T_{air} resulted in an
284 increase in forest productivity as GPP rose between 3.3-8.7 Mg C ha^{-1} yr^{-1} in all models
285 (Table 2).

286

287 **3.2 Leaf-scale responses**

Leaf-scale A_n and g_s oppose LAI responses; the model with the largest change in LAI in response to temperature increase (CLM3.5) has the lowest A_n values and the models with the smallest change in LAI (ED2, JULES & SiB3) have the greatest A_n values and the strongest responses of A_n to temperature change (Figure 4). Model uncertainty increases with temperature for A_n and V_{cmax} (Figure 4a & 5). For V_{cmax} this is caused by substantial variation in the optima (10˚C; Figure 5) and the rate of decline in V_{cmax} following the optima; in CLM3.5 V_{cmax} declines 50% at 9˚C over the optimum, contrasting with the same decline 17˚C over the optimum in SPA (Figure 5).

The optimum A_n in SPA, SiB3, JULES, CLM3.5 and ED2 occurs at T_{leaf} values of 25˚C, 26˚C, 27˚C, 30˚C and 30˚C respectively (Figure 4a) and significantly before the optimum point on V_{cmax} (Figure 5). In all models the A_n optimum and the initial decline in canopy average A_n is linked to declines in g_s (Figure 4a-b). Consequently for each model there are apparent, but variable, relationships between g_s and A_n (Figure 6), but no obvious relationships between A_n and V_{cmax} (Figure 7).

There was high variability in the magnitude and temperature response of g_s across the models. The maximum canopy average g_s values in SiB3 (486 mmol m^{-2} s^{-1} at 25˚C) and ED2 (384 mmol m^{-2} s^{-1} at 23˚C) are substantially higher than CLM3.5 (49 mmol m^{-2} s^{-1} at 20˚C), JULES (70 mmol m^{-2} s^{-1} at 25˚C) and SPA (200 mmol m^{-2} s^{-1} at 24˚C; Figure 4b). In CLM3.5 a strong constriction in *ET* is caused by the strong influence of β on g_s (Figure 4c-d). β is reduced by 85±31% in CLM3.5 as T_{leaf} increase from 30-40 ˚C. The decline in β over the same T_{leaf} range was only 14±1% in ED2, 38±5% in JULES and 7.9±1% in SiB3 (Figure 4d).

The slope of A_n against g_s indicates intrinsic water use efficiency (IWUE): the rate of increase

of assimilation per unit increase in g_s. If A_n is plotted against g_s separately for each model temperature simulations (-5˚C, 0˚C, +2˚C, +4˚C, +6˚C) and a linear fit is forced through the g_s and A_n data, it is apparent that all models simulate increasing IWUE (an increase in slope) from the -5˚C up to the +6˚C simulations (Figure 6 & Table 3). The increase in slope of A_n and g_s from the -5˚C to +6˚C temperature simulation is greater in the drought than control simulations in all models (Figure 6 & Table 3), suggesting that both increasing temperature and reduced water availability increase IWUE.

When the effect of soil water stress is removed and sunlit leaf level values are compared to the DG data for the models which could output separate sunlit leaf values of g_s and A_n (only SPA and CLM3.5; Figure 8), the peak A_n of sunlit leaves in SPA at 25˚C (8.72±0.24 μmol m^{-2} s^{-1}) is similar to the peak in the DG leaf-scale data at 30.5˚C (8.44±0.17 μmol m^{-2} s^{-1}; Figure 8a). In CLM3.5 the peak A_n at 29˚C is considerably higher (13.48±0.20 μmol m^{-2} s^{-1}), although it occurs at a similar temperature to the observed peak. Both CLM3.5 and SPA show a decline of A_n with temperature similar to the data. Modelled g_s, however, shows a poor match to the observations (Figure 8b). Peak g_s values occur at substantially lower T_{leaf} values in CLM3.5 (27˚C) and SPA (25˚C) than observed (33.5˚C; Figure 5b). The peak sunlit g_s in SPA are also significantly higher (434±88 mmol m^{-2} s^{-1}) than the observations (123±4 mmol m^{-2} s^{-1}) and show a very sharp decline not observed in the data (Figure 8b).

4 Discussion

4.1 Canopy- and leaf-scale feedbacks

331 The response of NEE and GPP to short-term changes in temperature demonstrated
332 substantially greater consistency across models than for LAI (Figure 2). Amongst the models
333 which had dynamic LAI, the change in LAI from the original value ranged from 4.5 m^2 m^{-2} in
334 SPA to 1.0 m^2 m^{-2} in ED2. Interestingly, the change of LAI with T_{air} in ED2 and JULES was
335 so low that it was more comparable to SiB3, a model with fixed LAI. This contrasts
336 CLMA3.5 and SPA, within which LAI declined substantially as T_{air} rose above a threshold
337 (Figure 2d). The inter-model range in LAI (maximum range 7.5 m^2 m^{-2}) was greater than the
338 decline in LAI with T_{air} in any model. If leaf-scale fluxes are scaled using an inaccurate LAI,
339 the simulation of both accurate leaf- and canopy-scale fluxes is not possible (Bonan et al.,
340 2012; Lloyd et al., 2010; Mercado et al., 2006; Mercado et al., 2009). Given the large
341 variability in LAI responses across the models, it would be expected that there should be a
342 greater variability in GPP and NEE than was observed. Therefore the models must
343 compensate for variability in canopy structural parameters, such as LAI, through adjustment
344 in other leaf-scale parameters if the observed consistency in ecosystem-scale responses is to
345 be maintained (Bonan *et al.,* 2012). We found substantial variation in the magnitude and
346 temperature responses of leaf-scale parameters: peak V_{cmax} had a 10˚C T_{leaf} range across the
347 models (Figure 5), g_s values varied by over an order of magnitude (Figure 4b), the inter-
348 model range of β and *ET* increased with T_{leaf} (Figure 4c-d), and there was a two-fold increase
349 in the inter-model range of A_n as T_{leaf} rose from 25-40˚C (Figure 4a). Such variability across
350 the models suggests that any similarity in the response of NEE to T_{air} among models is caused
351 by different processes and feedbacks at the leaf scale. Had the models been run to their
352 equilibrium states, it is likely that there would have been greater divergence of model
353 responses at both canopy- and leaf-scales. Prolonged higher temperatures reduce long-term

moisture availability and cause more severe changes in β; in dynamic PFT-models this can result in a substantial shift of PFT away from tropical forest. Without more data to evaluate which models produced the correct responses to temperature, it is hard to have confidence in predictions of climate change impacts in Amazonian. Variability in the control of g_s and leaf biochemistry on A_n and changes in IWUE efficiency with increasing temperature or drought will have significant consequences on the demand of water from a forest (Harper et al., 2014). In this study we find g_s had a greater control on the change in A_n with increasing temperature because: A_n started to decline at T_{leaf} values which were lower than those at which peak V_{cmax} occurred (Figure 4b and Figure 5) and A_n maintained a positive relationship with g_s across all models (Table 3; Figure 6), but no clear relationship with V_{cmax} (Figure 7). All the models in this study also predicted an increases in IWUE from the lowest (ambient T_{air} -5˚C) to the highest (ambient T_{air} +6˚C) temperature simulation; this increase in IWUE was also always greater in the drought temperature simulations relative to the control temperature simulations (Table 3; Figure 6). Increases in IWUE with increasing temperature suggests that as the ecosystem warms A_n will become more sensitive to reductions in g_s and g_s will maintain a greater control on A_n than biochemical controls, even at very extreme increases in temperature (ambient T_{air} +6˚C).

These results are consistent with the hypothesis that temperature increases will mainly be manifest through the effect of increased VPD on stomatal conductance (Lloyd and Farquhar 2008). They are also consistent with leaf warming data from the Tapajos forest which show that reductions in A_n start to occur at 4-5°C before the optimum point for V_{cmax} and J_{max} in sunlit leaves (Tribuzy, 2005). However the responses from longer-term leaf warming experiments at the same site showed that changes in leaf biochemistry with increasing leaf

377 temperatures was an important control on A_n (Doughty 2011), suggesting more data are
378 required to test effectively both the short and long term responses of A_n to changes in
379 temperature in models.

380 Comparing the short term direct effect of temperature on the A_n-g_s relationships is
381 complicated because of the differences in the calculation and implementation of the effect of
382 water stress amongst models (Powell et al., 2013; Zhou et al., 2013). β is altered by changes
383 in SWC, which can be caused by changes in temperature (via increased VPD altering SWC),
384 as well as changes in precipitation; in turn β alters both g_s (Figure S1) and A_n. The decrease
385 in β with temperature increase was highly variable among models (Figure 4d). Consequently,
386 the direct influence of soil water stress on g_s, A_n and *ET*, versus the indirect effect of VPD,
387 was inconsistent between models. Resolving these inconsistencies is important, as water
388 stress functions impact the ratio of modelled latent to sensible heat fluxes and so when
389 coupled to global climate models they alter climate and vegetation feedbacks (Harper et al.,
390 2014). Improving how water stress is simulated in models is therefore essential to improving
391 temperature and drought responses in tropical forests.

392 When focusing only on periods of high soil water content and therefore removing the effects
393 of water stress, A_n and g_s values from fully sunlit leaves still varied substantially from the
394 response and magnitude of the DG data (Figure 8). Given the DG data were averaged from
395 only three top-canopy species, some degree of variation between the model and the data is
396 expected. The variability between the peak data and peak model g_s was however > 4 times
397 (Figure 8b) and the modelled temperature optima for g_s (25-27˚C) was substantial lower than
398 observed by DG (33.5˚C).Given that CLM3.5 and SPA are in the lower range of the total

399 model variability for the g_s and A_n of an average canopy leaf (aggregated sunlit and shaded
400 leaf; Figure 4a-b), the variation from the data is likely to be substantially larger if sunlit leaf
401 data could be extracted from all models. Considering the importance of g_s in controlling leaf
402 productivity, the suitability of the empirical models of g_s used in these models requires
403 further testing (Bonan *et al.*, 2014). The use of optimised rather than empirical models may
404 provide an opportunity to improve the capability to simulate g_s responses to temperature and
405 water stress in greater detail (Heroult et al., 2013; Medlyn et al., 2013; Medlyn et al., 2011;
406 Zhou et al., 2013).

407

408 **4.2 Combined drought and temperature sensitivities**

409 Previous modelling studies have shown that there is high variability in how sensitive models
410 are to temperature and drought (Friedlingstein et al., 2006; Galbraith et al., 2010; Luo et al.,
411 2008; Sitch et al., 2008), but that vegetation models have embedded in them greater
412 sensitivity to rises in temperature than drought (Galbraith et al., 2010) despite the evidence
413 for strong drought sensitivity in natural rainforests (Gatti et al. 2014). The responses of
414 modelled forest production in this study to combined changes in precipitation and
415 temperature were however highly variable. CLM3.5 and SPA had very strong compound
416 effects of temperature on drought-induced reductions in GPP, R_{eco} and LAI (Figure 3)
417 relative to JULES and SiB3. In ED2, the drought effect on GPP was always stronger than the
418 temperature effect (Figure 3) because it has a strong drought-mortality effect at this site
419 (Powell et al., 2013). This study demonstrates that there is a continuum in model responses
420 from models that require a low increase in ambient T_{air} to cause the same GPP loss as a 50%

421 reduction in wet season rainfall (SPA, 4.9 ˚C), to models that have a very strong drought
422 response and therefore require a substantial increase in ambient T_{air} to replicate the same GPP
423 loss as a 50% reduction in wet season rainfall (ED2, 17.5 ˚C; Table 2). As a 6˚C rise in
424 temperature and a 50 % reduction in rainfall are changes which may occur in Amazonia
425 during the 21st century (Christensen et al, 2007; Collins et al., 2013), we suggest that there is
426 currently no consensus among vegetation models as to whether there will be a stronger
427 drought or temperature response to future climate change within tropical forests.

428 Across all the models GPP increased when ambient T_{air} was reduced by 5˚C; this occurred
429 because the ambient air temperature -5˚C was closer to the modelled g_s optima. This result
430 suggests models are currently predicting that Amazonian forests are operating beyond a
431 temperature and VPD optimum. Given that the models underestimate the point at which NEE
432 declines with T_{air} by 3-6˚C and the point at which g_s declines with T_{leaf} by 7.5-9.5˚C (Figure 2
433 and 4), it seems likely that the models in this study may be biased towards temperature
434 calibrations for temperate ecosystems. Consequently, as well as moving towards
435 implementing more mechanistic responses to improve models, more research to test and
436 adjust their temperature responses in tropical ecosystem is necessary. The range of model
437 responses in this study is likely to stem from real uncertainty in our understanding of the
438 responses by tropical rain forest ecosystems to changes in precipitation and temperature.
439 Further analysis of the same questions using models that vary in complexity (eg, statistical or
440 optimised models, as well as purely mechanistic) might provide additional insight into
441 mechanistic and simulation bias (systematic or random), as well advancing understanding
442 about climate risk that we derive from them (Meir, Mencuccini and Dewar, 2015)

5 Conclusion

This is the first study in which canopy and leaf temperature responses from multiple vegetation models are analysed and compared to existing data on leaf and canopy temperature responses from a tropical forest site. This study finds models lie along a continuum of those which have a greater sensitivity of GPP to changes in temperature relative to drought and those which have a greater sensitivity to drought relative to a change in temperature. Any consistency in model responses to temperature and drought were however, the result of inconsistent leaf-scale responses, which were found to compensate for substantial inter-model variation in the magnitude and response of LAI to drought and temperature.

All the models in this study predict that reductions in A_n are dominated by stomatal rather than biochemical responses and that IWUE increased with rising temperatures. The dominance of the effect of g_s rather than V_{cmax} on A_n results in all the models predicting greater forest productivity when temperatures are 5°C below ambient and closer the temperature of the g_s optimum. This suggests that currently models predict that tropical forests are operating beyond a temperature and VPD optimum, but we note that these predictions may be influenced by parameterisations derived originally from temperate zone forests.

This study concludes that to simulate effectively the response of the Amazon forest to changes in multiple climatic factors substantial improvements are needed in how leaf-scale processes and leaf-to-canopy scaling are simulated. Further observational data are also required to generate consistent leaf- and canopy-scale data for independent model evaluation.

Author Contributions

L. R. and M. W. designed the experiment, performed simulations, analysed data and prepared the manuscript. A. H., B. O. C., D. R. G., H. M. A. I., T. L. P., S. S, P. M. performed simulation, contributed to study design and prepared manuscript. D. D. contributed to the data analysis. N. L. and Y. M. contributed to the study design. P. M. contributed to data analysis and prepared the manuscript.

472 Acknowledgements

473 This research was enabled by a grant from the Andes-Amazon Initiative of The Gordon and
474 Betty Moore Foundation. L.R gratefully acknowledges financial support from the Natural
475 Environment Research Council (UK) for a NERC PhD studentship, and NERC grant
476 NE/J011002/1; PM also acknowledges support from ARC FT110100457. L.R would also like
477 to thank, L. Smallman and T. Hill for their help and support. L. Rowland would also like to
478 thank the reviewer Nicolas Delbart and the editor Hisashi Sato for their valuable contribution
479 to improving the quality of this manuscript.

480

481 References:

482 Baker, I. T., Prihodko, L., Denning, A. S., Goulden, M., Miller, S., and da Rocha, H. R.:
483 Seasonal drought stress in the Amazon: Reconciling models and observations, J Geophys
484 Res-Biogeo, 113, 2008.
485 Best, M. J., Pryor, M., Clark, D. B., Rooney, G. G., Essery, R. L. H., Menard, C. B.,
486 Edwards, J. M., Hendry, M. A., Porson, A., Gedney, N., Mercado, L. M., Sitch, S., Blyth, E.,
487 Boucher, O., Cox, P. M., Grimmond, C. S. B., and Harding, R. J.: The Joint UK Land
488 Environment Simulator (JULES), model description - Part 1: Energy and water fluxes,
489 Geosci Model Dev, 4, 677-699, 2011.
490 Bonan, G. B., Levis, S., Sitch, S., Vertenstein, M., and Oleson, K. W.: A dynamic global
491 vegetation model for use with climate models: concepts and description of simulated
492 vegetation dynamics, Global Change Biol, 9, 1543-1566, 2003.
493 Bonan, G. B., Oleson, K. W., Fisher, R. A., Lasslop, G., and Reichstein, M.: Reconciling leaf
494 physiological traits and canopy flux data: Use of the TRY and FLUXNET databases in the
495 Community Land Model version 4, Journal of Geophysical Research, 117, 2012.
496 Bonan, G. B., Williams, M., Fisher, R. A., and Oleson, K. W.: Modeling stomatal
497 conductance in the Earth system: linking leaf water-use efficiency and water transport along
498 the soil-plant-atmosphere continuum, Geosci. Model Dev. Discuss., 7, 3085-3159, 2014.
499 Brando, P. M., Nepstad, D. C., Davidson, E. A., Trumbore, S. E., Ray, D., and Camargo, P.:
500 Drought effects on litterfall, wood production and belowground carbon cycling in an Amazon
501 forest: results of a throughfall reduction experiment, Philos T R Soc B, 363, 1839-1848,
502 2008.
503 Christensen et al, J.: Regional Climate Projections. In: Climate Change 2007: the physical

504 science basis. Contribution of working group I to the Fourth Assessment Report of the
505 Intergovernmenatal Panel on Climate Change Solomon, S., Quin, D., Manning, M., Chen, Z.,
506 Marquies, M., Averyt, K., Tignor, M., and Miller, H. (Eds.), 1, Cambridge University Press,
507 Cambridge, UK; New York, NY, 2007.
508 Clark, D. B., Mercado, L. M., Sitch, S., Jones, C. D., Gedney, N., Best, M. J., Pryor, M.,
509 Rooney, G. G., Essery, R. L. H., Blyth, E., Boucher, O., Harding, R. J., Huntingford, C., and
510 Cox, P. M.: The Joint UK Land Environment Simulator (JULES), model description - Part 2:
511 Carbon fluxes and vegetation dynamics, Geosci Model Dev, 4, 701-722, 2011.
512 Collatz, G. J., Ball, J. T., Grivet, C., and Berry, J. A.: Physiological and Environmental-
513 Regulation of Stomatal Conductance, Photosynthesis and Transpiration - a Model That
514 Includes a Laminar Boundary-Layer, Agricultural and Forest Meteorology, 54, 107-136,
515 1991.
516 Collins, M., Knutti, R., Arblaster, J., Dufresne, J.-L., Fichefet, T., Friedlingstein, P., Gao, X.,
517 Gutowski, W. J., Johns, T., Krinner, G., Shongwe, M., Tebaldi, C., A.J., W., and Wehner, M.:
518 Long-term Climate Change: Projections, Comitments and Irreversibility In: Climate Change
519 2013: The Physical Science Basis Contribution of Working Group I to the Fifth Assessment
520 Report of the Intergovernmental Panel on Climate Change [Stocker, T.F., D. Qin, G.-K.
521 Plattner, M. Tignor, S.K. Allen, J. Boschung, A. Nauels, Y. Xia, V. Bex and P.M. Midgley
522 (eds.)], Cambridge University Press, Cambridge, United Kingdon and New York, NY USA,
523 2013.
524 Corlett, R. T.: Impacts of warming on tropical lowland rainforests, Trends Ecol Evol, 26,
525 606-613, 2011.
526 Cox, P. M., Harris, P. P., Huntingford, C., Betts, R. A., Collins, M., Jones, C. D., Jupp, T. E.,

527 Marengo, J. A., and Nobre, C. A.: Increasing risk of Amazonian drought due to decreasing
528 aerosol pollution, Nature, 453, 212-215, 2008. doi:10.1038/nature06960
529 Cox, P. M., Huntingford, C., and Harding, R. J.: A canopy conductance and photosynthesis
530 model for use in a GCM land surface scheme, J Hydrol, 212, 79-94, 1998.
531 da Costa, A. C. L., Galbraith, D., Almeida, S., Portela, B. T. T., da Costa, M., Silva, J. D.,
532 Braga, A. P., de Goncalves, P. H. L., de Oliveira, A. A. R., Fisher, R., Phillips, O. L.,
533 Metcalfe, D. B., Levy, P., and Meir, P.: Effect of 7 yr of experimental drought on vegetation
534 dynamics and biomass storage of an eastern Amazonian rainforest, New Phytol, 187, 579-
535 591, 2010. doi: 10.1111/j.1469-8137.2010.03309
536 da Costa, A. C. L., Metcalfe, D. B., Doughty, C. E., de Oliveira, A. A. R., Neto, G. F. C., da
537 Costa, M. C., Silva, J. D., Aragao, L. E. O. C., Almeida, S., Galbraith, D. R., Rowland, L. M.,
538 Meir, P., and Malhi, Y.: Ecosystem respiration and net primary productivity after 8-10 years
539 of experimental through-fall reduction in an eastern Amazon forest, Plant Ecol Divers, 7, 7-
540 24, 2014.
541 Doughty, C. E.: An In Situ Leaf and Branch Warming Experiment in the Amazon,
542 Biotropica, 43, 658-665, 2011.
543 Doughty, C. E. and Goulden, M. L.: Are tropical forests near a high temperature threshold?,
544 Journal of Geophysical Research, 113, 2008.
545 Farquhar, G. D., Caemmerer, S. V., and Berry, J. A.: A Biochemical-Model of Photosynthetic
546 Co2 Assimilation in Leaves of C-3 Species, Planta, 149, 78-90, 1980.
547 Farquhar, G. D. and Sharkey, T. D.: Stomatal Conductance and Photosynthesis, Annual
548 Review of Plant Physiology and Plant Molecular Biology, 33, 317-345, 1982.
549 Fisher, R. A., Williams, M., Da Costa, A. L., Malhi, Y., Da Costa, R. F., Almeida, S., and

550 Meir, P.: The response of an Eastern Amazonian rain forest to drought stress: results and
551 modelling analyses from a throughfall exclusion experiment, Global Change Biol, 13, 2361-
552 2378, 2007.
553 Fisher, R. A., Williams, M., Do Vale, R. L., Da Costa, A. L., and Meir, P.: Evidence from
554 Amazonian forests is consistent with isohydric control of leaf water potential, Plant Cell and
555 Environment, 29, 151-165, 2006.
556 Friedlingstein, P., Cox, P., Betts, R., Bopp, L., Von Bloh, W., Brovkin, V., Cadule, P.,
557 Doney, S., Eby, M., Fung, I., Bala, G., John, J., Jones, C., Joos, F., Kato, T., Kawamiya, M.,
558 Knorr, W., Lindsay, K., Matthews, H. D., Raddatz, T., Rayner, P., Reick, C., Roeckner, E.,
559 Schnitzler, K. G., Schnur, R., Strassmann, K., Weaver, A. J., Yoshikawa, C., and Zeng, N.:
560 Climate-carbon cycle feedback analysis: Results from the C(4)MIP model intercomparison,
561 Journal of Climate, 19, 3337-3353, 2006.
562 Gatti, L. V., Gloor, M., Miller, J. B., Doughty, C. E., Malhi, Y., Domingues, L. G., Basso, L.
563 S., Martinewski, A., Correia, C. S. C., Borges, V. F., Freitas, S., Braz, R., Anderson, L. O.,
564 Rocha, H., Grace, J., Phillips, O. L., and Lloyd, J.: Drought sensitivity of Amazonian carbon
565 balance revealed by atmospheric measurements, Nature, 506, 76, 2014.
566 doi:10.1038/Nature12957
567 Galbraith, D., Levy, P. E., Sitch, S., Huntingford, C., Cox, P., Williams, M., and Meir, P.:
568 Multiple mechanisms of Amazonian forest biomass losses in three dynamic global vegetation
569 models under climate change, New Phytol, 187, 647-665, 2010.
570 Good, P., Jones, C., Lowe, J., Betts, R., and Gedney, N.: Comparing Tropical Forest
571 Projections from Two Generations of Hadley Centre Earth System Models, HadGEM2-ES
572 and HadCM3LC, Journal of Climate, 26, 495-511, 2013.

573 Goudriaan, J.: Crop micrometeorology: A simulation study. , Center for Agricultural
574 Publishing and Documentation, Wageningen, The Netherlands., 1977.
575 Goulden, M. L., Miller, S. D., da Rocha, H. R., Menton, M. C., de Freitas, H. C., Figueira, A.
576 M. E. S., and de Sousa, C. A. D.: Diel and seasonal patterns of tropical forest CO2 exchange,
577 Ecological Applications, 14, S42-S54, 2004.
578 Harper, A., Baker, I. T., Denning, A. S., Randall, D. A., Dazlich, D., and Branson, M.:
579 Impact of Evapotranspiration on Dry Season Climate in the Amazon Forest, J Climate, 27,
580 574-591, 2014.
581 Heroult, A., Lin, Y. S., Bourne, A., Medlyn, B. E., and Ellsworth, D. S.: Optimal stomatal
582 conductance in relation to photosynthesis in climatically contrasting Eucalyptus species under
583 drought, Plant Cell Environ, 36, 262-274, 2013.
584 Jupp, T. E., Cox, P. M., Rammig, A., Thonicke, K., Lucht, W., and Cramer, W.:
585 Development of probability density functions for future South American rainfall, New
586 Phytol, 187, 682-693, 2010.
587 Kim, Y., Knox, R. G., Longo, M., Medvigy, D., Hutyra, L. R., Pyle, E. H., Wofsy, S. C.,
588 Bras, R. L., and Moorcroft, P. R.: Seasonal carbon dynamics and water fluxes in an Amazon
589 rainforest, Global Change Biol, 18, 1322-1334, 2012.
590 Kirschbaum, M. U. F. and Farquhar, G. D.: Temperature-Dependence of Whole-Leaf
591 Photosynthesis in Eucalyptus-Pauciflora Sieb Ex Spreng, Australian Journal of Plant
592 Physiology, 11, 519-538, 1984.
593 Levis, S., Bonan, G., Vertenstein, M., and Oleson, K.: The Community Land Model Dynamic
594 Global Vegetation Model (CLM-DGVM): technical description and user's guide., Boulder,
595 CO, USA: National Center for Atmospheric Research., 2004.

596 Lloyd, J. and Farquhar, G. D.: Effects of rising temperatures and [CO2] on the physiology of
597 tropical forest trees, Philos Trans R Soc Lond B Biol Sci, 363, 1811-1817, 2008.
598 Lloyd, J., Patino, S., Paiva, R. Q., Nardoto, G. B., Quesada, C. A., Santos, A. J. B., Baker, T.
599 R., Brand, W. A., Hilke, I., Gielmann, H., Raessler, M., Luizao, F. J., Martinelli, L. A., and
600 Mercado, L. M.: Optimisation of photosynthetic carbon gain and within-canopy gradients of
601 associated foliar traits for Amazon forest trees, Biogeosciences, 7, 1833-1859, 2010.
602 Luo, Y., Gerten, D., Le Maire, G., Parton, W. J., Weng, E., Zhou, X., Keough, C., Beier, C.,
603 Ciais, P., Cramer, W., Dukes, J. S., Emmett, B., Hanson, P. J., Knapp, A., Linder, S.,
604 Nepstad, D. A. N., and Rustad, L.: Modeled interactive effects of precipitation, temperature,
605 and [CO2] on ecosystem carbon and water dynamics in different climatic zones, Global
606 Change Biol, 14, 1986-1999, 2008.
607 Malhi, Y., Aragao, L. E., Galbraith, D., Huntingford, C., Fisher, R., Zelazowski, P., Sitch, S.,
608 McSweeney, C., and Meir, P.: Exploring the likelihood and mechanism of a climate-change-
609 induced dieback of the Amazon rainforest, Proc Natl Acad Sci U S A, 106, 20610-20615,
610 2009.
611 Marengo, J. A., Chou, S. C., Kay, G., Alves, L. M., Pesquero, J. F., Soares, W. R., Santos, D.
612 C., Lyra, A. A., Sueiro, G., Betts, R., Chagas, D. J., Gomes, J. L., Bustamante, J. F., and
613 Tavares, P.: Development of regional future climate change scenarios in South America using
614 the Eta CPTEC/HadCM3 climate change projections: climatology and regional analyses for
615 the Amazon, So Francisco and the Parana River basins, Climate Dynamics, 38, 1829-1848,
616 2012.
617 Marengo, J. A., J. Tomasella, L. M. Alves, W. R. Soares, and D. A. Rodriguez.: The drought
618 of 2010 in the context of historical droughts in the Amazon region, Geophys. Res. Lett., 38,

619 L12703, doi:10.1029/2011GL047436.
620 Mcmurtrie, R. E., Leuning, R., Thompson, W. A., and Wheeler, A. M.: A Model of Canopy
621 Photosynthesis and Water-Use Incorporating a Mechanistic Formulation of Leaf Co2
622 Exchange, Forest Ecology and Management, 52, 261-278, 1992.
623 Medlyn, B. E., Duursma, R. A., De Kauwe, M. G., and Prentice, I. C.: The optimal stomatal
624 response to atmospheric CO2 concentration: Alternative solutions, alternative interpretations,
625 Agr Forest Meteorol, 182, 200-203, 2013.
626 Medlyn, B. E., Duursma, R. A., Eamus, D., Ellsworth, D. S., Prentice, I. C., Barton, C. V. M.,
627 Crous, K. Y., de Angelis, P., Freeman, M., and Wingate, L.: Reconciling the optimal and
628 empirical approaches to modelling stomatal conductance, Global Change Biol, 17, 2134-
629 2144, 2011.
630 Medvigy, D., Wofsy, S. C., Munger, J. W., Hollinger, D. Y., and Moorcroft, P. R.:
631 Mechanistic scaling of ecosystem function and dynamics in space and time: Ecosystem
632 Demography model version 2, Journal of Geophysical Research, 114, 2009a.
633 Medvigy, D., Wofsy, S. C., Munger, J. W., Hollinger, D. Y., and Moorcroft, P. R.:
634 Mechanistic scaling of ecosystem function and dynamics in space and time: Ecosystem
635 Demography model version 2, Journal of Geophysical Research-Biogeosciences, 114, 2009b.
636 Meir, P., Metcalfe, D. B., Costa, A. C., and Fisher, R. A.: The fate of assimilated carbon
637 during drought: impacts on respiration in Amazon rainforests, Philosophical transactions of
638 the Royal Society of London. Series B, Biological sciences, 363, 1849-1855, 2008.
639 Meir, P. and Woodward, F. I.: Amazonian rain forests and drought: response and
640 vulnerability, New Phytologist, 187, 553-557, 2010.
641 Meir, P., Mencuccini. M., and Dewer. R. C. Tree mortality during drought: narrowing the

642 gaps in understanding and prediction, New Phytologist, in press.
643 Mercado, L., Lloyd, J., Carswell, F., Malhi, Y., Meir, P., and Nobre, A. D.: Modelling
644 Amazonian forest eddy covariance data: a comparison of big leaf versus sun/shade models
645 for the C-14 tower at Manaus I. Canopy photosynthesis, Acta Amazonica, 36, 69-82, 2006.
646 Mercado, L. M., Lloyd, J., Dolman, A. J., Sitch, S., and Patino, S.: Modelling basin-wide
647 variations in Amazon forest productivity - Part 1: Model calibration, evaluation and upscaling
648 functions for canopy photosynthesis, Biogeosciences, 6, 1247-1272, 2009.
649 Moorcroft, P. R., Hurtt, G. C., and Pacala, S. W.: A method for scaling vegetation dynamics:
650 The ecosystem demography model (ED), Ecological Monographs, 71, 557-585, 2001.
651 Nepstad, D. C., Moutinho, P., Dias, M. B., Davidson, E., Cardinot, G., Markewitz, D.,
652 Figueiredo, R., Vianna, N., Chambers, J., Ray, D., Guerreiros, J. B., Lefebvre, P., Sternberg,
653 L., Moreira, M., Barros, L., Ishida, F. Y., Tohlver, I., Belk, E., Kalif, K., and Schwalbe, K.:
654 The effects of partial throughfall exclusion on canopy processes, aboveground production,
655 and biogeochemistry of an Amazon forest, Journal of Geophysical Research-Atmospheres,
656 107, 2002.
657 Oleson, K. W., Dai, Y., Bonan, G. B., Bosilovich, M., Dirmeyer, P., Hoffman, F., Levis, S.,
658 Niu, G. Y., Thornton, P. E., Vertenstein, M., Yang, Z. L., and Zeng, X.: Technical description
659 of the Community Land Model (CLM), NCAR Technical Note, 2004.
660 Oleson, K. W., Niu, G. Y., Yang, Z. L., Lawrence, D. M., Thornton, P. E., Lawrence, P. J.,
661 Stockli, R., Dickinson, R. E., Bonan, G. B., Levis, S., Dai, A., and Qian, T.: Improvements to
662 the Community Land Model and their impact on the hydrological cycle, J Geophys Res-
663 Biogeo, 113, 2008.
664 Powell, T. L., Galbraith, D. R., Christoffersen, B. O., Harper, A., Imbuzeiro, H. M., Rowland,

665 L., Almeida, S., Brando, P. M., da Costa, A. C., Costa, M. H., Levine, N. M., Malhi, Y.,
666 Saleska, S. R., Sotta, E., Williams, M., Meir, P., and Moorcroft, P. R.: Confronting model
667 predictions of carbon fluxes with measurements of Amazon forests subjected to experimental
668 drought, New Phytol, 2013.
669 Reed, S. C., Wood, T. E., and Cavaleri, M. A.: Tropical forests in a warming world, New
670 Phytologist, 193, 27-29, 2012.
671 Reichstein, M., Bahn, M., Ciais, P., Frank, D., Mahecha, M.D., Seneviratne, S.I.,
672 Zscheischler, J., Beer, C., Buchmann, N., Frank, D.C., Papale, D., Rammig, A., Smith, P.,
673 Thonicke, K., van der Velde, M., Vicca, S., Walz, A., Wattenbach, M. (2013) Climate
674 extremes and the carbon cycle. Nature 500, 287-295. doi 10.1038/Nature12350
675 Sellers, P. J.: Canopy Reflectance, Photosynthesis and Transpiration, Int J Remote Sens, 6,
676 1335-1372, 1985.
677 Sellers, P. J., Berry, J. A., Collatz, G. J., Field, C. B., and Hall, F. G.: Canopy Reflectance,
678 Photosynthesis, and Transpiration .3. A Reanalysis Using Improved Leaf Models and a New
679 Canopy Integration Scheme, Remote Sensing of Environment, 42, 187-216, 1992.
680 Sellers, P. J., Randall, D. A., Collatz, G. J., Berry, J. A., Field, C. B., Dazlich, D. A., Zhang,
681 C., Collelo, G. D., and Bounoua, L.: A revised land surface parameterization (SiB2) for
682 atmospheric GCMs .1. Model formulation, Journal of Climate, 9, 676-705, 1996.
683 Sitch, S., Huntingford, C., Gedney, N., Levy, P. E., Lomas, M., Piao, S. L., Betts, R., Ciais,
684 P., Cox, P., Friedlingstein, P., Jones, C. D., Prentice, I. C., and Woodward, F. I.: Evaluation
685 of the terrestrial carbon cycle, future plant geography and climate-carbon cycle feedbacks
686 using five Dynamic Global Vegetation Models (DGVMs), Global Change Biol, 14, 2015-
687 2039, 2008.

688 Tribuzy, E. S.: Variações da temperatura foliar do dossel e o seu efeito na taxa assimilatória
689 de CO2 na Amazônia Central, PhD, Universidade de São Paulo, São Paulo, 2005.
690 Williams, M.: A three-dimensional model of forest development and competition, Ecological
691 Modelling, 89, 73-98, 1996.
692 Williams, M., Malhi, Y., Nobre, A. D., Rastetter, E. B., Grace, J., and Pereira, M. G. P.:
693 Seasonal variation in net carbon exchange and evapotranspiration in a Brazilian rain forest: a
694 modelling analysis, Plant Cell and Environment, 21, 953-968, 1998.
695 Williams, M., Schwarz, P. A., Law, B. E., Irvine, J., and Kurpius, M. R.: An improved
696 analysis of forest carbon dynamics using data assimilation, Global Change Biol, 11, 89-105,
697 2005.
698 Wood, T. E., Cavaleri, M. A., and Reed, S. C.: Tropical forest carbon balance in a warmer
699 world: a critical review spanning microbial- to ecosystem-scale processes, Biol Rev Camb
700 Philos Soc, 87, 912-927, 2012.
701 Zhou, S. X., Duursma, R. A., Medlyn, B. E., Kelly, J. W. G., and Prentice, I. C.: How should
702 we model plant responses to drought? An analysis of stomatal and non-stomatal responses to
703 water stress, Agr Forest Meteorol, 182, 204-214, 2013.
704 Zhou, X. H., Weng, E. S., and Luo, Y. Q.: Modeling patterns of nonlinearity in ecosystem
705 responses to temperature, CO2, and precipitation changes, Ecological Applications, 18, 453-
706 466, 2008.

707

708 Table 1: Summary of the characteristics of each of the five vegetation models (CLM3.5,
709 ED2, JULES, SiB3, & SPA).

710

	CLM3.5	**ED2**	**JULES**	**SiB3**	**SPA**
No° of plant function types	5	4	10	1	1
Canopy structure	Big-leaf	Gap model	Layered Canopy	Big-leaf	Layered canopy
Leaf Area index	Dynamic	Dynamic	Dynamic	Fixed	Dynamic
Division of sunlit and shaded leaf	Y (discrete division)	N	N	N	Y (discrete division)
Simulation of water stress on A_n and g_s.	Water stress factor	Water stress factor	Water stress factor	Water stress factor	Linked soil-leaf water potential/resistance model to g_s model.
Origin of photosynthesis model	Farquhar et al., (1980); Farquhar and Sharkey (1982); Collatz et al. (1991)	Farquhar et al., (1980); Farquhar and Sharkey (1982); Collatz et al. (1991)	Farquhar et al., (1980); Farquhar and Sharkey (1982); Collatz et al. (1991)	Farquhar et al., 1(980); Farquhar and Sharkey (1982) Collatz et al. (1991)	Farquhar et al., (1980); Kirschbaum and Farquhar (1984); McMurtrie et al. (1992)
Key model references	Bonan et al., (2003); Levis et al., (2004); Oleson et al. (2008).	Medvigy et al., (2009); Kim et al 2012.	Best et al., (2011); Clark et al., (2011)	Sellers et al., (1992); Sellers et al., (1996); Baker et al (2008).	Williams, (1996); Williams et al., (2005); Fisher et al., (2006)

711

712

713

714

715 Table 2: Model values for GPP (Mg C ha^{-1} yr^{-1}) for the last year (2006) of the ambient air
716 temperature control plot simulation (T_{air} +0°C), the control plot simulation -5°C (T_{air} -5°C),
717 the control plot simulation +6°C (T_{air} +6°C) and the ambient air temperature drought plot
718 simulation (T_{air} +0°C). The equivalent temperature is the elevation in the control plot
719 simulation temperature needed to replicate the same magnitude reduction in GPP as the
720 drought simulation, for the year 2006 and at ambient temperatures. The equivalent
721 temperature is derived from a linear relationship between GPP values in 2006 and the air
722 temperatures in the 5 temperature simulations per model.

723

724

	CLM3.5	ED2	JULES	SiB3	SPA
Control GPP T_{air} -5°C	40.74	31.74	36.73	35.27	38.23
Control GPP T_{air} +0°C	36.68	28.31	31.16	31.95	29.55
Control GPP T_{air} +6°C	28.03	20.70	20.08	27.50	15.89
Drought GPP T_{air} +0°C	26.47	10.79	18.13	20.86	19.55
Equivalent T_{air}	8.83	17.50	8.61	15.70	4.92

725 Table 3: Values show the normalised intrinsic water use efficiency (IWUE) calculated from
726 the linear slope of normalised A_n plotted against normalised g_s (Figure 6). The normalised
727 IWUE is calculated separately for each models' control and drought temperature simulations
728 (ambient air temperature (T_{air}) -5˚C, +0 ˚C, +2 ˚C,+4 ˚C, and +6 ˚C). [Note NA in CLM3.5
729 drought simulations indicates the model changed from a forest to a grassland]

730

	Control Simulations					Drought Simulations				
	CLM3.5	ED2	JULES	SiB3	SPA	CLM3.5	ED2	JULES	SiB3	SPA
T_{air} -5˚C	0.84	0.42	0.50	0.09	0.49	0.73	0.29	0.50	0.10	0.27
T_{air} +0˚C	0.93	0.56	0.83	0.49	0.68	0.93	0.40	0.60	0.93	0.24
T_{air} +2˚C	1.01	0.67	1.01	0.58	0.73	1.08	0.53	0.97	1.11	0.41
T_{air} +4˚C	1.05	0.79	1.18	0.65	1.00	NA	0.78	1.37	1.20	0.74
T_{air} +6˚C	1.11	0.95	1.32	0.69	1.50	NA	1.10	1.73	1.22	1.15

731

732 Figure captions:

733 Figure 1: Schematic diagram showing how droughts, via the combined effects of increased
734 air temperature (T) and reduced precipitation (PPT), affect the carbon cycle of a tropical
735 forest, including the effects on: vapour pressure deficit (VPD), evapo-transpiration (E_t),
736 stomatal conductance (g_s), soil water content (SWC), net photosynthesis (A_n), leaf area index
737 (LAI), the maximum rates of RuBP carboxylation and electron transport (V_{cmax} and J_{max}
738 respectively), autotrophic respiration (R_a) heterotrophic respiration (R_h), gross primary
739 productivity (GPP), and net ecosystem exchange (NEE). + signs indicates a positive feedback
740 effect between variables (i.e. an increase in one variable can only cause an increase in another
741 if all else is equal), - signs indicate a negative feedback effect, and +/- indicate the possibility
742 of both a positive and negative effect. Solid arrows represent responses which occur over
743 short timescales of minutes to hours, whereas dashes arrows represent responses which can
744 occur over longer timescales from days to months.

745 Figure 2: Comparison of the air temperature (T_{air} °C) response of a) daytime net ecosystem
746 exchange (NEE, μmol m^{-2} s^{-1} ; note that negative values of NEE indicate carbon
747 sequestration), b) gross primary productivity (GPP, μmol m^{-2} s^{-1}), c) ecosystem respiration
748 (R_{eco} (μmol m^{-2} s^{-1}), d) leaf area index (LAI, m^2 m^{-2}). The lines show the median model
749 responses from the five control temperature runs per model pooled and divided into 1°C
750 temperature bins. The grey shaded area shows the combined 15.9th and 84.1th quantiles for all
751 models. The black points and error bars in panel a) show the daytime eddy-flux inferred NEE
752 (cf. Figure 4 in Doughty and Goulden 2008).

753 Figure 3: Modelled effect of short-term changes in temperature and drought. Changes in: a)

754 gross primary productivity (GPP) b) ecosystem respiration (R_{eco}) and c) leaf area index
755 (LAI) in the final year (2006) in the drought run expressed as a fraction of the value in the
756 final year (2006) of the control run, for the T_{air} -5˚C (grey bars) and T_{air} +6˚C (white bars)
757 simulations.

758 Figure 4: Comparison of the dry season mean (sunlit + shaded leaves, weighted by their
759 respective LAIs) leaf-level response to temperature ($T_{leaf;}$ °C) of a) net photosynthesis (A_n,
760 μmol m^{-2} s^{-1}), b) stomatal conductance (g_s, mmol m^{-2} s^{-1}), c) leaf transpiration (E_t, mm m^{-2} s^{-1}), and d) the soil water stress factor (β) for average canopy leaves [Note SPA does not
762 simulate β] . The lines show the median model responses from the control plot for the five
763 temperature simulations pooled and divided into 1 °C temperature bins for each model. The
764 grey shaded area shows the combined 15.9th and 84.1th quantiles for all models. [Note JULES
765 Et data is missing from these simulations]

766 Figure 5: The temperature response of V_{cmax} for each model shown relative to the V_{cmax} at
767 25 °C per model.

768 Figure 6: The relationship between 30 minute values of modelled stomatal conductance (g_s)
769 and photosynthesis (A_n) normalised by their respective maximum values; A_n and g_s values are
770 taken only from the dry season when PPFD > 1000 μmol m^{-2} s^{-1} . Values are coloured
771 separately from deep blue to red (see legend) for each temperature simulations (ambient air
772 temperature -5˚C, +0 ˚C,+2 ˚C,+4 ˚C, and +6 ˚C) and panels separate the control (panels a-e)
773 and drought simulations (panels f-j), for each model. Values are from sunlit and shaded
774 leaves, weighted by their respective LAIs. A separate linear line is plotted through the
775 normalised A_n, g_s data for each temperature simulations, the slope of which represents the

776 normalised intrinsic water use efficiency: the normalised increase in A_n per unit increase in
777 normalised g_s. Linear lines are also coloured from deep blue to deep red to differentiate the
778 additions to ambient air temperature (see legend).

779 Figure 7: The relationship between V_{cmax} (μmol m^{-2} s^{-1}) and photosynthesis (A_n mmol m^{-2} s^{-1})
780 for the half hourly output from each model in the dry season of the control runs, with PPFD >
781 1000 μmol m^{-2} s^{-1}. Values are from sunlit and shaded leaves, weighted by their respective
782 LAIs. Results are shown across all leaf temperatures explored in this study (colour change
783 from blue to red indicates increasing leaf temperature (see legend).

784 Figure 8: The sunlit leaf-level response of dry season a) net photosynthesis (A_n, μmol m^{-2} s^{-1})
785 and b) stomatal conductance (g_s, μmol m^{-2} s^{-1}) to leaf temperature ($T_{leaf;}$ °C) for CLM3.5
786 (orange) and SPA (red). The lines show the median model responses from the control plot for
787 the five temperature simulations pooled and divided into 1 °C temperature bins for each
788 model. The shaded areas around each line show the 15.9^{th} and 84.1^{th} quantiles for each
789 model. Data from Doughty and Goulden is shown as black points; error bars show the
790 standard error. [Note only SPA and CLM3.5 output data on sunlit leaf values of A_n and g_s.]
791

792 Figure S1: The relationship between β and stomatal conductance (g_s mmol m^{-2} s^{-1}) for each
793 model in the dry season, with PPFD > 1000 μmol m^{-2} s^{-1}. Values are from sunlit and shaded
794 leaves, weighted by their respective LAIs. Results are shown across all leaf temperatures
795 explored in this study (colour change from blue to red indicated increasing leaf temperature)
796 and separately for the drought and control simulation.

797

798 Figure 1:

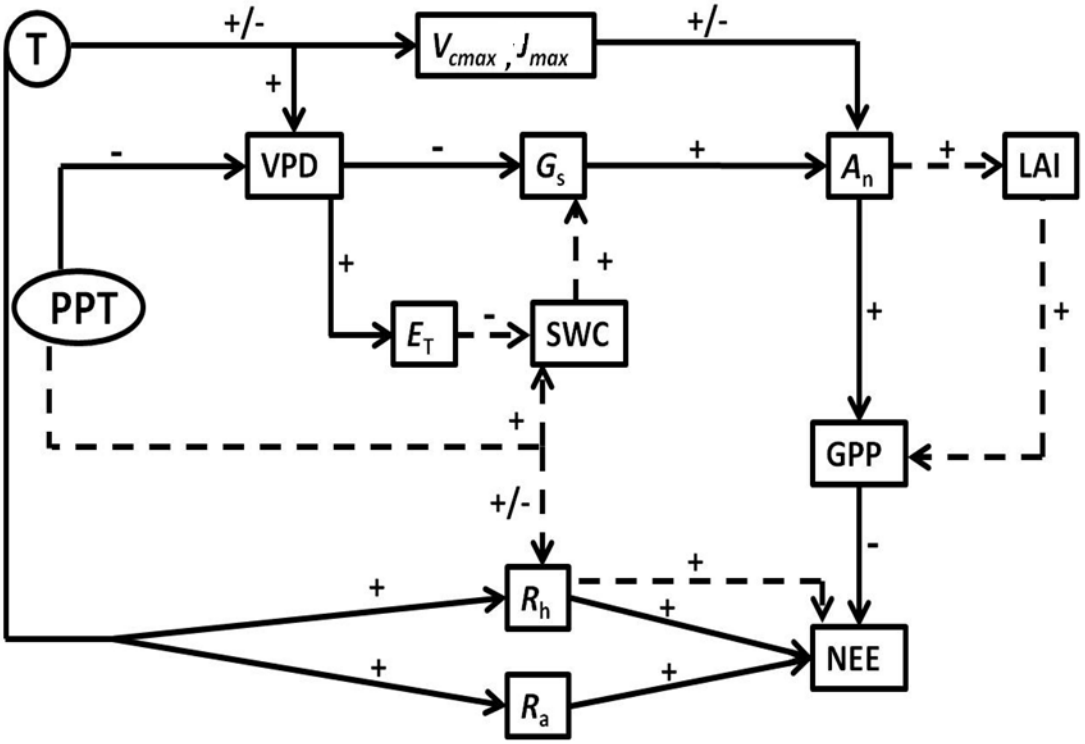

799

800

801 Figure 2:

802

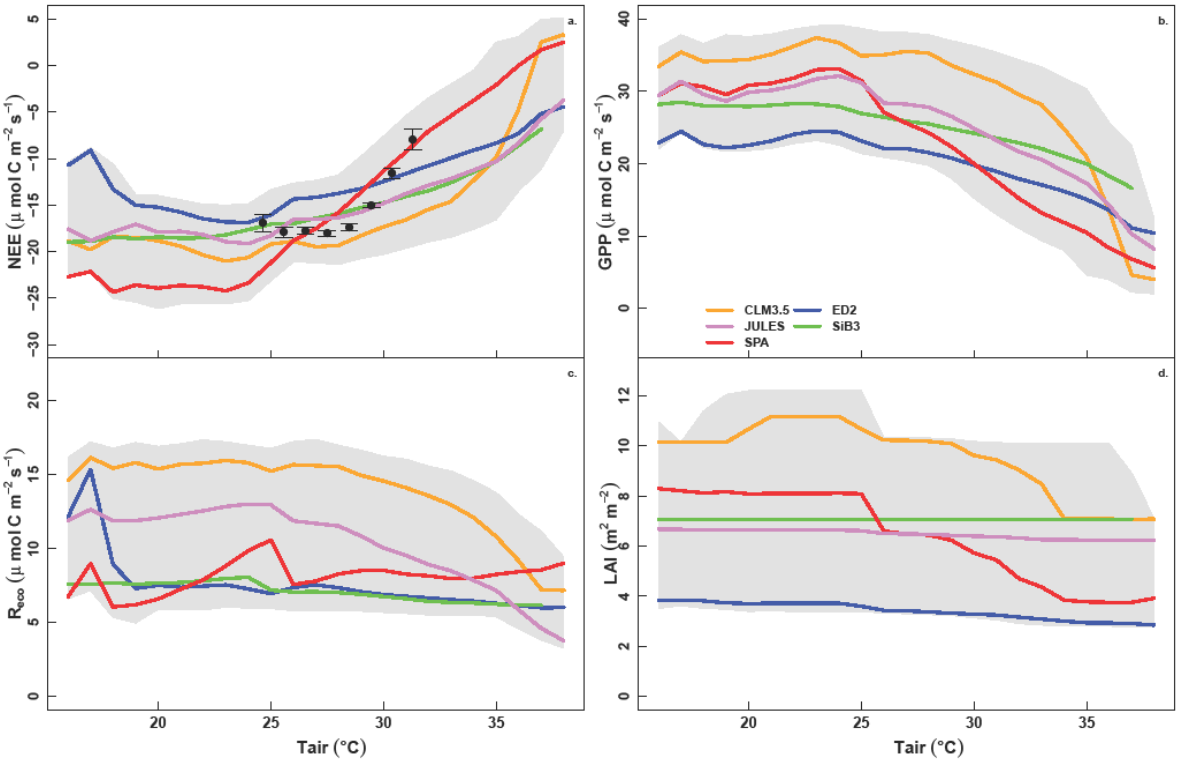

803
804

805

806 Figure 3

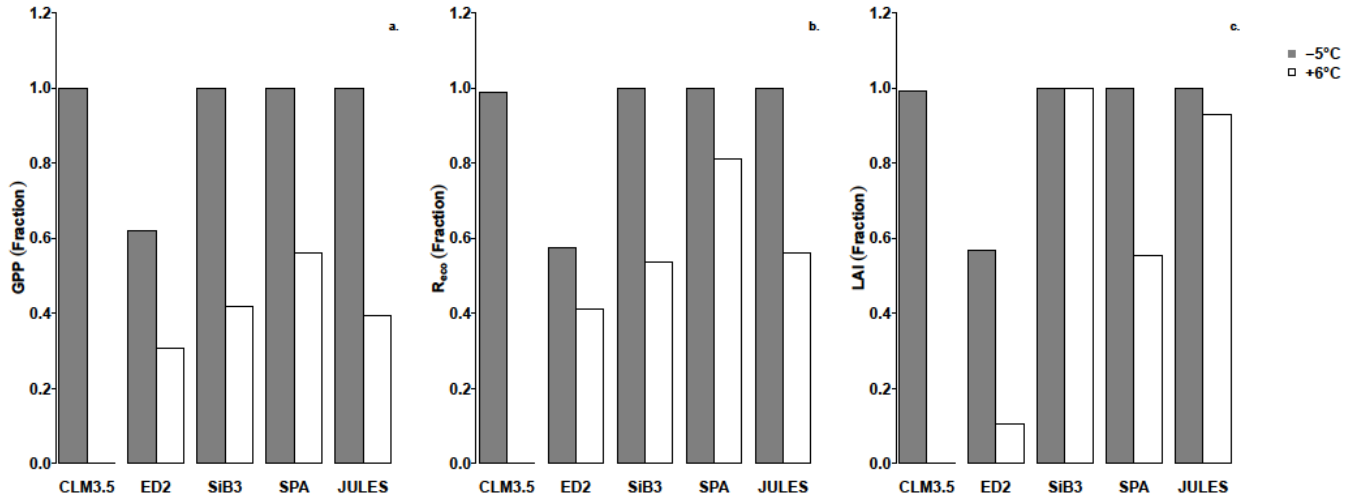

807
808

809

810 Figure 4:

811

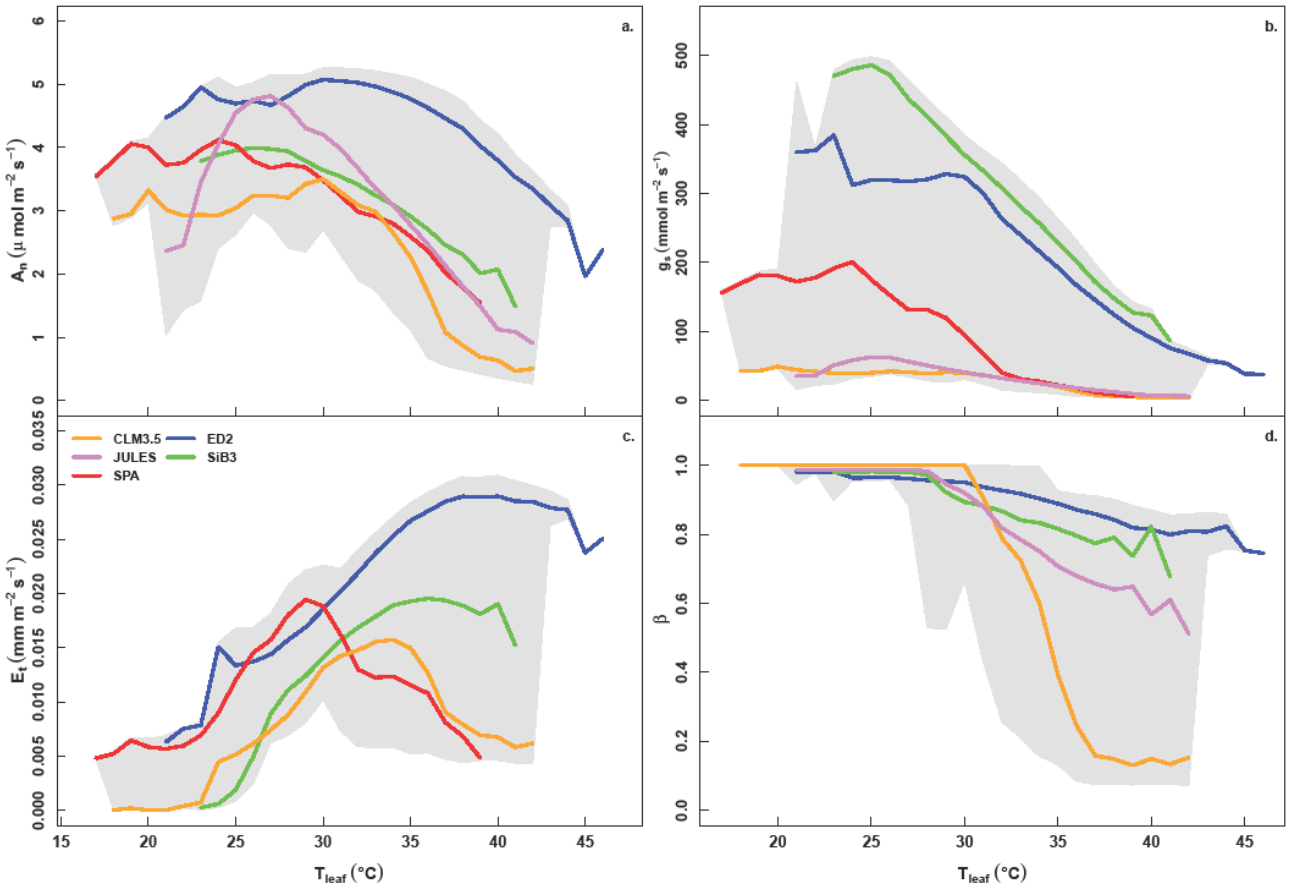

812
813

814 Figure 5:

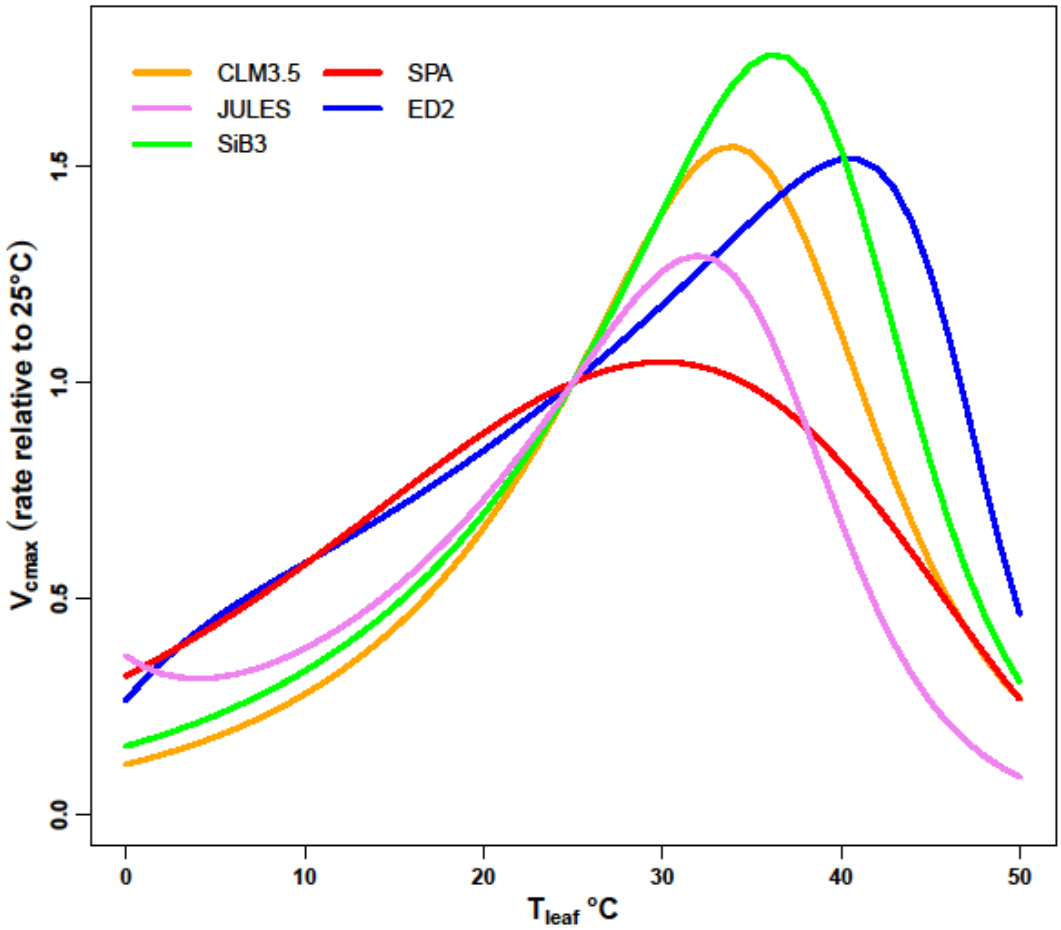

815

816

817

818

819

820

821

822

823

Figure 6:

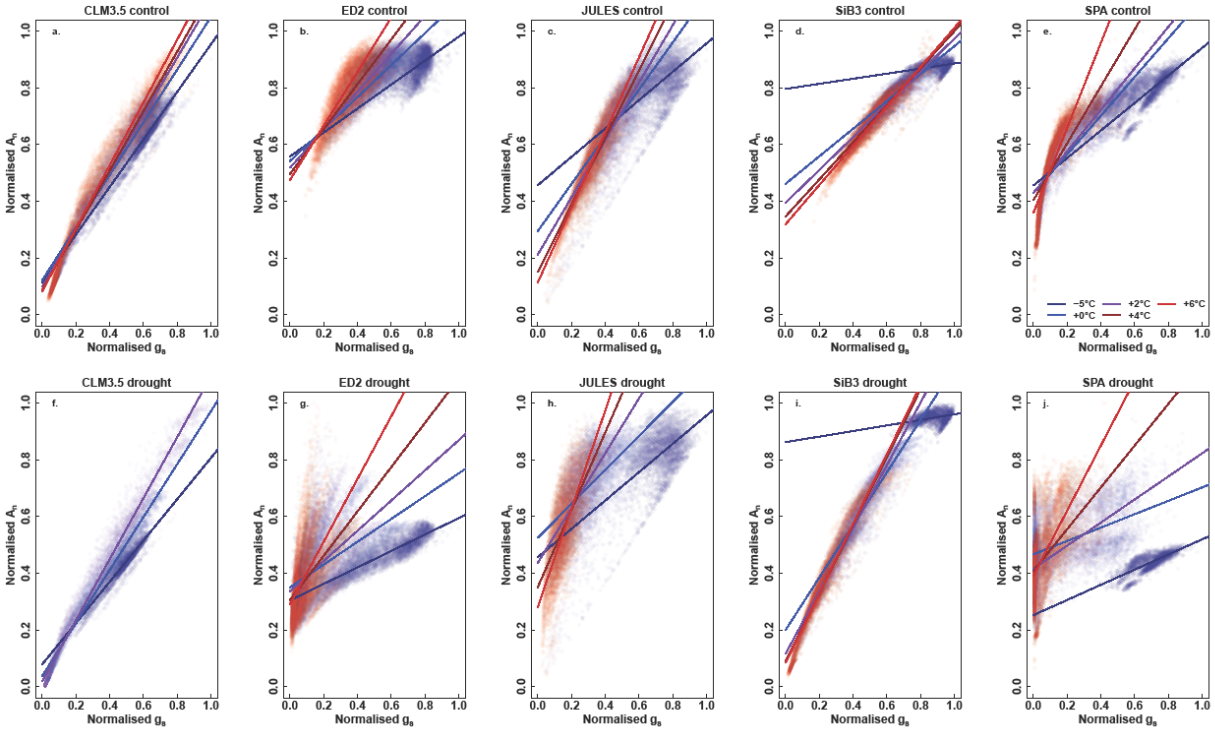
CLM3.5 control
ED2 control
JULES control
SiB3 control
SPA control
CLM3.5 drought
ED2 drought
JULES drought
SiB3 drought
SPA drought
Normalised A_n
Normalised g_s
−5°C
+0°C
+2°C
+4°C
+6°C

828 Figure 7:

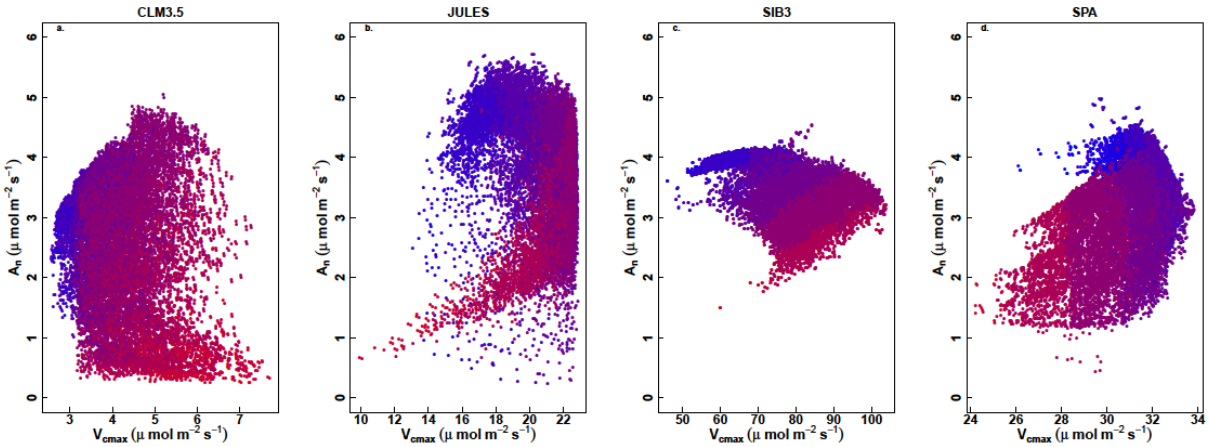

829
830

831

832 Figure 8:

833

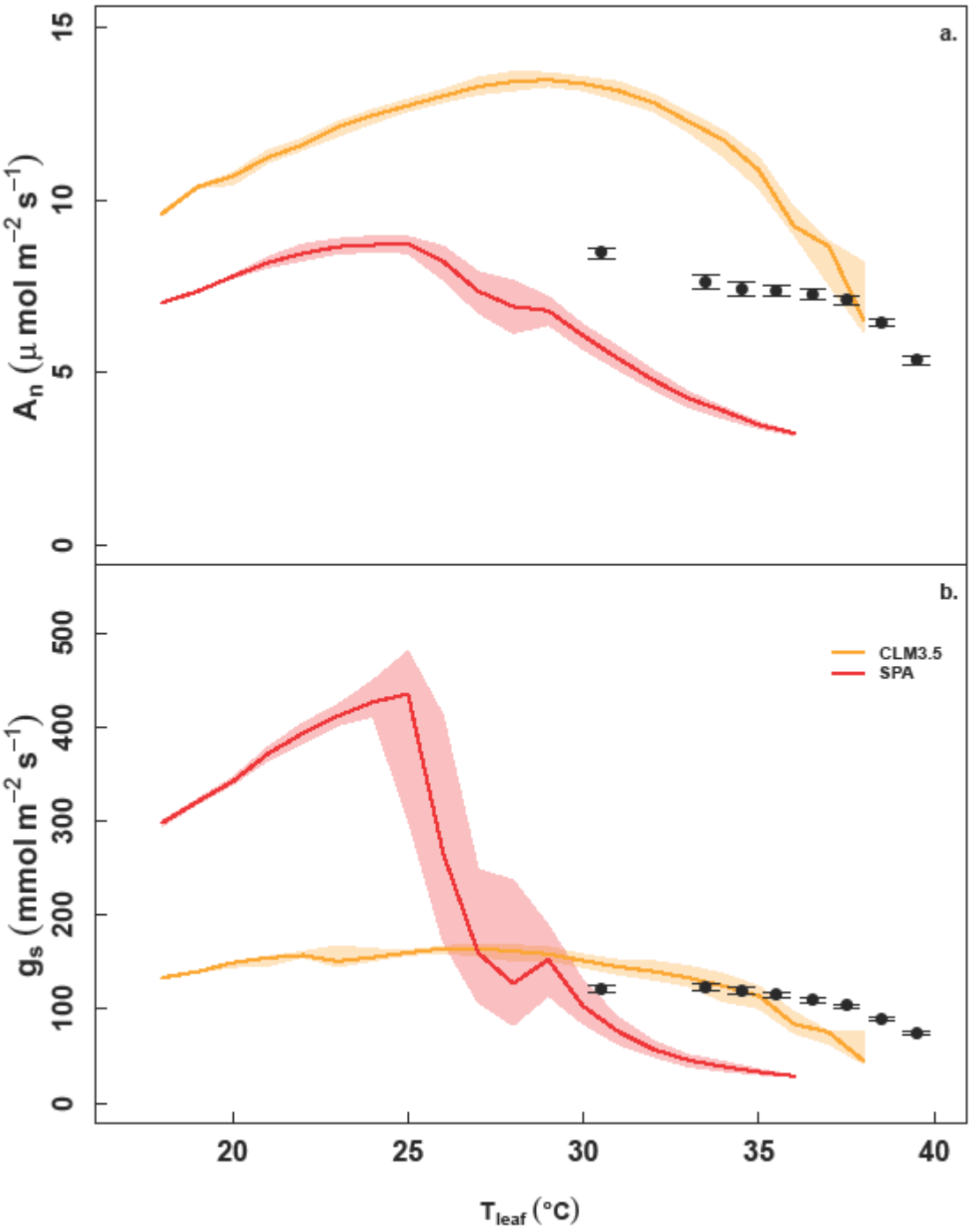

834
835

836

837 Figure S1:

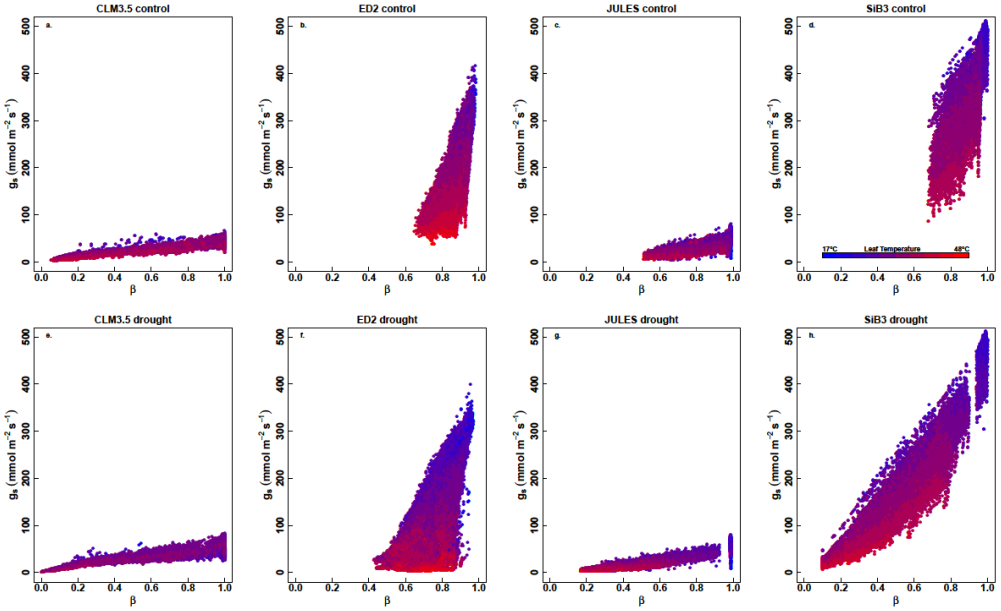

838